HYDROGEN, FUEL CELL & ENERGY STORAGE

Thermo-Economic Analysis of a Geothermal-based Multigeneration System Using the Kalina Cycle for Power, Heating, Cooling, Hydrogen and Freshwater Production

Arkan Jabbar Farhan Farhan | Majid Abbasalizadeh*
Shahram Khalilarya | Samad Jafarmadar

Faculty of Mechanical Engineering, University of Urmia, Iran
* Corresponding author, Email: m.abbasalizadeh@urmia.ac.ir

Article Information

Article Type
Research Article

Article History
Received: *28 Oct 2025*
Revised: *15 Dec 2025*
Accepted: *14 Feb 2026*
Published Online: *08 Mar 2026*

Keywords
Geothermal energy
Kalina cycle
Multigeneration system
Thermo-economic analysis
Hydrogen production

Abstract

This study presents an in-depth thermodynamic and economic evaluation of a hybrid geothermal energy system utilizing Kalina cycle technology for multipurpose power generation. The system is designed to produce electricity and heating while supplying cooling, hydrogen, and freshwater. The integrated system reaches a total energy efficiency of 47.6% and an exergy efficiency of 44.2%. Raising the high pressure setting in the Kalina cycle to 4900 kPa reduces the exergy destruction cost rate to \$1486.49/h, the total cost rate to \$2464.12/h, and the capital investment rate to \$922.12/h, compared to the base pressure of 4000 kPa where these rates were \$1912.08/h for exergy destruction and \$3084.00/h for total cost and \$1171.92/h for capital investment. The exergetic assessment shows Turbine 2 and the Compressor as the main contributors to system exergy destruction, with outputs of 2545.33 kW and 2353.09 kW, respectively. At a rate of 0.1524 kg/h the system establishes two operational capabilities: hydrogen production and a cooling output of 3498 kW. The research indicates that the combined multigeneration system enhances resource utilization ofgeothermal energy by maximizing energy efficiency and decreasing operational costs.

Cite this article: Farhan, A. J. F., Abbasalizadeh, M., Khalilarya, S., Jafarmadar, S. (2026). Thermo-Economic Analysis of a Geothermal-based Multigeneration System Using the Kalina Cycle for Power, Heating, Cooling, Hydrogen and Freshwater Production. DOI: 10.22104/hfe.2025.7588.1356

 Publisher: Iranian Research Organization for Science and Technology (IROST)
DOI: 10.22104/hfe.2025.7588.1356

1 Introduction

Global attention has increasingly turned toward renewable technologies due to rising resource consumption and growing demands for environmental sustainability. Among these alternatives, geothermal energy stands out for its consistent energy supply, broad accessibility, and environmentally friendly energy production [1]. Geothermal power plants, extracting Earth's internal heat, have become core renewable energy systems which produce both electricity and heat distribution. Regular power plants restrict their geothermal resource utilization because they produce only a single form of energy. The combination of multiple energy output systems into single unit serves as a promising approach to enhancing efficiency while cutting down on waste production. These systems transform waste heat from primary energy generation into secondary energy forms which optimize the whole process performance. A promising system links geothermal power to Kalina cycle, using an ammonia-water mixture as working fluid. Research have proven that this cycle outperforms traditional Rankine cycles, specifically for geothermal applications utilizing low to moderate temperature heat sources [2]. Geothermal-based systems that use the Kalina cycle enable various applications including heating and cooling by absorption technologies, electrolysis hydrogen production and freshwater desalination. These multigeneration systems demonstrate high versatility by resolving multiple energy and resource difficulties simultaneously [3]. While the technical potential of geothermal multigeneration systems has been widely recognized, comprehensive thermo-economic analyses of these systems remain limited. Thermo-economic analysis is essential for evaluating the efficiency and economic feasibility of multigeneration systems, as it integrates thermodynamic modeling with financial assessment to optimize their large-scale implementation [4].

This review will examine geothermal multigeneration system research together with similar systems' thermo-economic evaluations to identify prevailing developments, current barriers, and unmet research needs. Ślusarczyk and Ziółkowski [5] evaluate low-enthalpy geothermal resources for electricity generation using ORC and Kalina Cycle applications. The researchers evaluated the thermodynamic operation of both systems under geothermal conditions across a temperature range of 100°C to 180°C. Research findings show that Kalina Cycles yield 15% higher power generation, especially when processing lower temperature geothermal sources between 100°C-130°C. Under matching geothermal conditions, the Kalina Cycle generated an electrical efficiency of 10.5% while the ORC achieved 8.2%. Hai et al. [6] conducted an extensive performance examination of an innovative combined geothermal system which unites an enhanced Organic Rankine Cycle (ORC) with a dual-turbine Kalina Cycle, together with reverse osmosis desalination and supercritical CO_2 cycles. The single-flash geothermal source enables this system to simultaneously produce electricity, heat, and freshwater. The study carried out energy and exergy analyses, as well as exergoeconomic assessments. The base configuration produced a total power output of 130.068 MW while reaching an energy efficiency of 46.08% and an exergy efficiency of 56.04%, along with heating load of 30.79 MW and freshwater production of 44.97 kg/s.

Yuksel et al. [7] conducted a study to evaluate the viability of geothermal-powered multigeneration facilities which use the Kalina cycle to produce cooling, electricity, and hydrogen. The system functions with low-temperature geothermal resources through which it combines reverse osmosis desalination with thermoelectric generators. The study demonstrates an energy efficiency of 46.87% and an exergy efficiency of 44.13%. The greatest exergy destruction occurs within the Kalina cycle, while the exergy efficiency for liquid hydrogen production reaches 54.17%. Bahrami and Rosen [8] conducted an exergoeconomic assessment combined with multi-objective optimization of a geothermal-powered zero-emission system for cooling, electricity generation, and hydrogen production. The system utilizes a half-effect absorption chiller together with an Organic Rankine cycle (ORC) and a Proton Exchange Membrane (PEM) electrolyzer. When operating at 80 °C source temperature, the system reaches optimal exergy and energy efficiencies of 48% and 19.5%, respectively. Musharavati, Ahmadi and Khanmohammadi [9] analyzed a hybrid geothermal power plant integrating an ORC with absorption refrigeration and PEM electrolysis. Under ideal circumstances, the system reached thermal and exergy efficiency rates of 72% and 43.2% respectively. The optimal system design obtained through multi-objective optimization maximized electricity production at 4.8 MW while minimizing the overall cost of clean hydrogen production. Researchers found that this geothermal-based trigeneration system is financially competitive and environmentally safe, making it an effective approach for geothermal multigeneration applications.

Ambriz-Díaz et al. [10] carried out a performance appraisal of the low-emissions multi-generation system based on geothermal cascade, using exergoeconomic and exergoenvironmental assessments alongside energy and exergy analyses. The highest hierarchical system stage reached 83% for energy efficiency and 48% for

exergy efficiency. The exergoeconomic evaluation revealed that system electricity production had a cost rate of $0.065 per kilowatt hour. Environmental analysis results showed that facilities using this system produced 72% fewer carbon dioxide emissions compared to those relying on conventional fossil fuels. Xu et al. [11] analyzed the thermodynamic, exergoeconomic, and exergoenvironmental performance of a new geothermal trigeneration system built to power a sports arena. The implemented system achieved 78% thermal efficiency with 42% exergy efficiency. Optimization analysis showed that the system could generate 5 MW of electricity, 3 MW of cooling power, and 2 MW of heating capacity, while achieving minimum hydrogen production costs of $0.09 per kilogram. Based on exergoeconomic analysis, the total system capital expenses can be recovered within 6.5 years which generates a net present value (NPV) of $2.3 million during twenty years. The power plant developed by Kelem and Yilmaz [12] utilizes geothermal resources to generate electricity while producing heat, freshwater, and compressed hydrogen through their multi-energy production features. The thermodynamic assessment together with economic modeling confirmed 70.1% energy efficiency and 47.8% exergy efficiency. During operation, this system generates 4.6 kg of hydrogen and 560 liters of freshwater every day. Geothermal integration for multi-use energy production proves both practicality and sustainability through a 5.5-year short payback period and favorable net present value calculations.

The review introduces multi-generation systems based on renewable geothermal energy, examining technologies which enables power production, heating and cooling, hydrogen generation and freshwater supply. Although the combined use of Kalina cycle and ORC and transcritical refrigeration and absorption refrigeration systems has received attention, a comprehensive thermodynamic and thermoeconomic analysis of these integrated systems is still lacking. This study is innovative because it investigates hydrogen production together with freshwater generation by using geothermal power alongside LNG heat sinks prioritizing sustainability, operational efficiency and cost-effectiveness. The combined method generates valuable performance advantages for energy systems.

2 System Modeling and Description

Figure 1 presents the schematic diagram of the multi-generation system configuration which the analysis focuses on. The schematic diagram provides an in-depth view of the integrated energy system under investigation. The main power generation relies on geothermal methods that employ enhanced thermodynamic cycles which operate in combination with subsystem components. The system combines elements such as Kalina flash cycle, Organic Rankine Cycle (ORC), LNG regasification, single-effect absorption refrigeration, transcritical refrigeration, Proton Exchange Membrane (PEM) electrolyzer, and reverse osmosis (RO) desalination. The multi-generation system produces electricity, heating, cooling, hydrogen, and water, thereby enhancing its overall sustainability. It illustrates how subsystems interact through operational relationships and introduces the evaluation framework, based on thermoeconomic analysis, which is used for performance evaluation in the following sections.

Evaluating system performance requires both exergy analysis and cost assessments of exergy destruction within each system component. Understanding the costs associated with exergy destruction allows optimization of operational efficiency and economic performance. System design becomes is enhanced by integrating the combination of exergy flow costs with investment and operational costs within an economic exergy analysis. The approach requires maintaining balance between input and output expenses per component by taking into account fuel expenses and the costs of the produced outputs. Efficiency depends on exergy destruction costs because lower exergoeconomic factors indicate greater exergy losses and help guide efforts to reduce expenses while improving system performance. The equations used to analyze the system from exergoeconomic point of view are as follows [4,13]:

$$\dot{C}_i = c_i \dot{\mathrm{Ex}}_i \,, \tag{1}$$

$$\dot{C}_W = c_W \dot{W} \,, \tag{2}$$

$$\dot{C}_q = c_q \dot{\mathrm{Ex}}_q \,, \tag{3}$$

$$\sum \left(c_{\mathrm{out}}\, \dot{\mathrm{Ex}}_{\mathrm{out}}\right)_k + c_{w,k}\dot{W}_k = c_{q,k}\dot{\mathrm{Ex}}_{q,k} + \sum \left(c_{\mathrm{in}}\, \dot{\mathrm{Ex}}_{\mathrm{in}}\right)_k + \dot{Z}_k \,, \tag{4}$$

$$\dot{Z}_k = \frac{Z_k \times \varphi \times \mathrm{CRF}}{\tau} \,, \tag{5}$$

$$\mathrm{CRF} = \frac{i_r(1+i_r)^n}{(1+i_r)^n - 1} \,, \tag{6}$$

$$c_{F,k} = \frac{\dot{C}_{F,k}}{\dot{E}_{F,k}} \,, \tag{7}$$

$$\dot{C}_{D,k} = c_{F,k}\dot{E}_{D,k} \,, \tag{8}$$

$$f_k = \frac{\dot{Z}_k}{\dot{Z}_k + \dot{C}_{D,k}} \,. \tag{9}$$

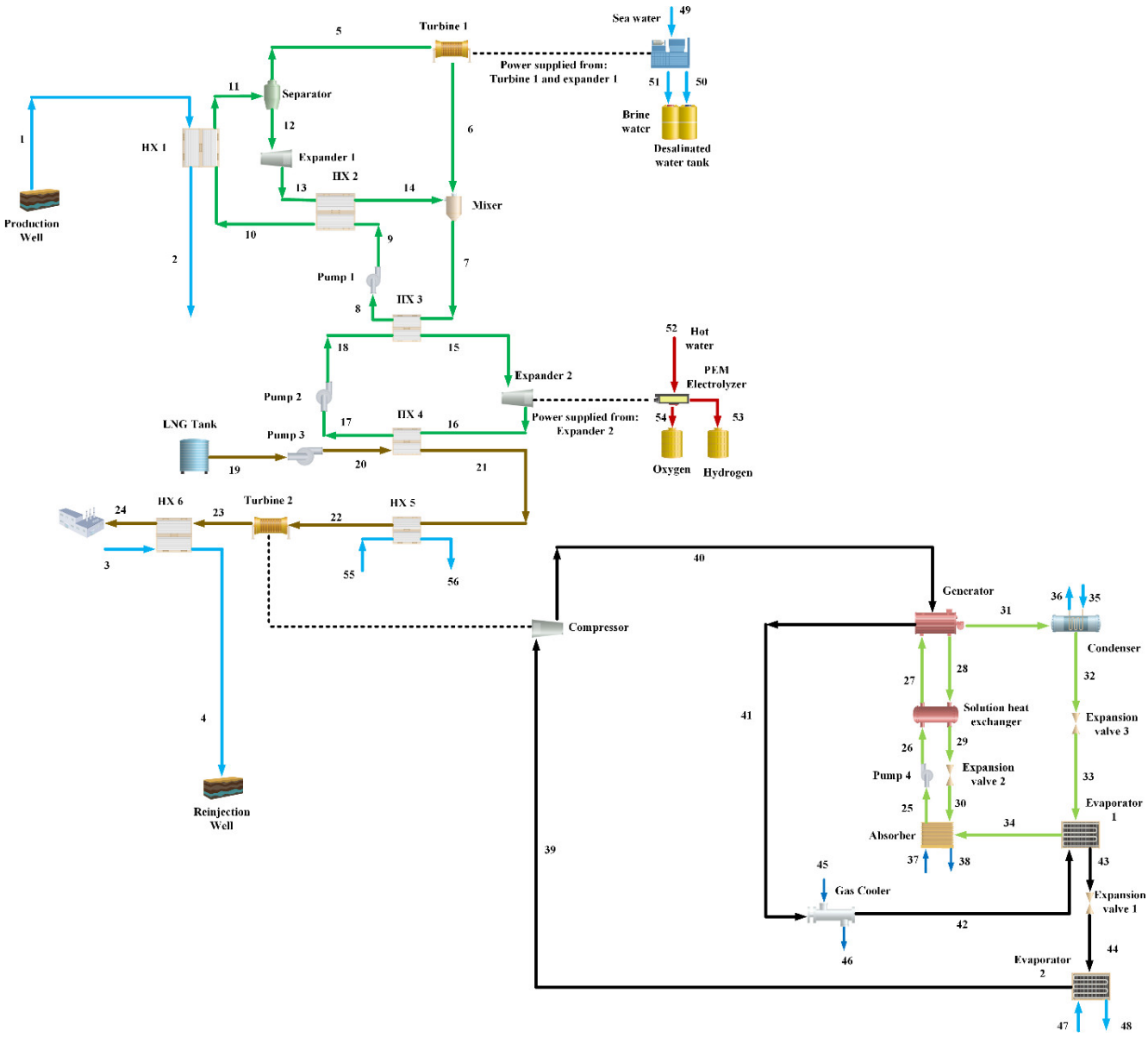

Fig. 1. The Schematic of geothermal based multigeneration system

Table 1 presents key thermoeconomic system analysis formulas, which calculate energy conversion costs, exergy destruction, and capital expenses. By integrating thermodynamic and economic calculations, the system allows for continuous cost evaluations, enabling performance-based strategies to minimize costs and improve system accuracy from installation to operation.

The proposed system analysis distributes financial costs through cost balance equations together with exergy flow cost rates to determine how system expenses ought to be distributed across the whole system. The established technique provides exact thermoeconomic evaluations by optimizing performance and enabling guided improvement decisions.

3 Results and Discussion

3.1 Validation of thermodynamic models

Kalina cycle validation. The Kalina cycle validation procedure involved comparing simulation results obtained from the developed code with the published data of Ji-chao and Sobhani [17]. The simulation showed excellent agreement for key performance metrics such as temperature and enthalpy at various points, as detailed in Table 3. Minor discrepancies observed are attributed to differences in boundary conditions

and operating parameters; however, all results remain within acceptable margins. This validation confirms that the simulation model reliably represents the actual behavior of the Kalina cycle under the studied conditions.

Table 1. Cost balance equations for system components formulated through thermoeconomic analysis [14–16]

Component	Function of purchase cost ($)
Heat exchanger	$Z_{\mathrm{HX}} = 2143\, A^{0.514}$
Turbine	$Z_{\mathrm{turb}} = 4405\, (\dot{W}_{\mathrm{turb}})^{0.7}$
Pump	$Z_{\mathrm{pump}} = 1120\, (\dot{W}_{\mathrm{pump}})^{0.8}$
Expander	$Z_{\mathrm{Exp}} = 3143.7 + 21743 \dot{V}_{\mathrm{out}}$
Evaporator	$Z_{\mathrm{eva}} = 1397 A_{\mathrm{eva}}^{0.89}$
Compressor	$Z_{\mathrm{comp}} = \dfrac{44.71 m_1 \times r_p^{\mathrm{comp}} \times \ln\left(r_p^{\mathrm{comp}}\right)}{0.95 - \eta_{\mathrm{is}}^{\mathrm{comp}}}$
Gas cooler	$Z_{\mathrm{GC}} = 1300 \left(\dfrac{A_{\mathrm{GC}}}{0.93}\right)^{0.78}$
Generator	$Z_{\mathrm{gen}} = 17500\, (A_{\mathrm{gen}})^{0.514}$
Condenser	$Z_{\mathrm{con}} = 1773\, \dot{m}_{\mathrm{cond}}$
Expansion valve	$Z_{\mathrm{exv}} = 114.5\, \dot{m}_{\mathrm{exv}}$
PEM	$Z_{\mathrm{PEM}} = 1000\, (\dot{W}_{\mathrm{PEM}})$
RO	$Z_{\mathrm{RO}} = n_e n_p c_k + n_p c_p + 996 (\dot{m}_{50})^{0.8}$

Table 2. Cost balance and auxiliary equations for the components of the analyzed system

Kalina cycle		
Heat exchanger 1	$\dot{C}_1 + \dot{C}_{10} + \dot{Z}_{\mathrm{HX1}} = \dot{C}_7 + \dot{C}_{11}$	$c_1 = c_2$
Separator	$\dot{C}_{11} + \dot{Z}_{\mathrm{sep}} = \dot{C}_5 + \dot{C}_{12}$	$c_5 = c_{12}$
Turbine 1	$\dot{C}_5 + \dot{Z}_{\mathrm{turb1}} = \dot{C}_6 + \dot{C}_{w,\mathrm{turb1}}$	$c_5 = c_6$
Expander 1	$\dot{C}_{12} + \dot{Z}_{\mathrm{Exp1}} = \dot{C}_{13} + \dot{C}_{w,\mathrm{Exp1}}$	$c_{12} = c_{13}$
Heat exchanger 2	$\dot{C}_{13} + \dot{C}_9 + \dot{Z}_{\mathrm{HX2}} = \dot{C}_{14} + \dot{C}_{10}$	$c_9 = c_{10}$
Mixer	$\dot{C}_6 + \dot{C}_{14} + \dot{Z}_{\mathrm{mix}} = \dot{C}_7$	–
Heat exchanger 3	$\dot{C}_7 + \dot{C}_{18} + \dot{Z}_{\mathrm{HX3}} = \dot{C}_8 + \dot{C}_{15}$	$c_7 = c_8$
Pump 1	$\dot{C}_9 = \dot{Z}_{\mathrm{pump1}} + \dot{C}_8 + \dot{C}_{w,\mathrm{pump1}}$	$c_{w,\mathrm{pump1}} = c_{w,\mathrm{turb1}}$
ORC cycle		
Pump 2	$\dot{C}_{18} = \dot{Z}_{\mathrm{pump2}} + \dot{C}_{17} + \dot{C}_{w,\mathrm{pump2}}$	$c_{w,\mathrm{pump2}} = c_{w,\mathrm{Exp2}}$
Expander 2	$\dot{C}_{15} + \dot{Z}_{\mathrm{Exp2}} = \dot{C}_{16} + \dot{C}_{w,\mathrm{Exp2}}$	$c_{15} = c_{16}$
Heat exchanger 4	$\dot{C}_{16} + \dot{C}_{20} + \dot{Z}_{\mathrm{HX4}} = \dot{C}_{17} + \dot{C}_{21}$	$c_{16} = c_{17}$
LNG system		
Pump 3	$\dot{C}_{20} = \dot{Z}_{\mathrm{pump3}} + \dot{C}_{19} + \dot{C}_{w,\mathrm{pump3}}$	$c_{w,\mathrm{pump3}} = c_{w,\mathrm{turb2}}$
Heat exchanger 5	$\dot{C}_{21} + \dot{C}_{55} + \dot{Z}_{\mathrm{HX5}} = \dot{C}_{22} + \dot{C}_{56}$	$c_{21} = c_{22},\ c_{55} = 0$
Turbine 2	$\dot{C}_{22} + \dot{Z}_{\mathrm{turb2}} = \dot{C}_{23} + \dot{C}_{w,\mathrm{turb2}}$	$c_{22} = c_{23}$
Heat exchanger 6	$\dot{C}_{23} + \dot{C}_3 + \dot{Z}_{\mathrm{HX6}} = \dot{C}_{24} + \dot{C}_4$	$c_{23} = c_{24}$
Transcritical refrigeration system		
Evaporator 2	$\dot{C}_{44} + \dot{C}_{47} + \dot{Z}_{\mathrm{eva2}} = \dot{C}_{39} + \dot{C}_{48}$	$c_{44} = c_{39},\ c_{47} = 0$
Compressor	$\dot{C}_{39} + \dot{C}_{w,\mathrm{comp}} + \dot{Z}_{\mathrm{comp}} = \dot{C}_{40}$	–
Gas cooler	$\dot{C}_{41} + \dot{C}_{45} + \dot{Z}_{\mathrm{GC}} = \dot{C}_{42} + \dot{C}_{46}$	$c_{41} = c_{42},\ c_{45} = 0$
Evaporator 1	$\dot{C}_{33} + \dot{C}_{42} + \dot{Z}_{\mathrm{eva1}} = \dot{C}_{34} + \dot{C}_{43}$	$c_{33} = c_{34}$
Expansion valve 1	–	$c_{43} = c_{44}$

Table 2. (*Continued*)

Absorption refrigeration system		
Absorber	$\dot{C}_{30}+\dot{C}_{34}+\dot{C}_{37}+\dot{Z}_{\text{abs}}=\dot{C}_{25}+\dot{C}_{38}$	$c_{37}=0,\ \dfrac{\dot{C}_{30}+\dot{C}_{34}}{\dot{\text{Ex}}_{30}+\dot{\text{Ex}}_{34}}=c_{25}$
Generator	$\dot{C}_{40}+\dot{C}_{27}+\dot{Z}_{\text{gen}}=\dot{C}_{41}+\dot{C}_{28}+\dot{C}_{31}$	$c_{40}=c_{41},\ \dfrac{\dot{C}_{28}-\dot{C}_{27}}{\dot{\text{Ex}}_{28}-\dot{\text{Ex}}_{27}}=\dfrac{\dot{C}_{31}-\dot{C}_{27}}{\dot{\text{Ex}}_{31}-\dot{\text{Ex}}_{27}}$
Condenser	$\dot{C}_{31}+\dot{C}_{35}+\dot{Z}_{\text{cond}}=\dot{C}_{32}+\dot{C}_{36}$	$c_{31}=c_{32},\ c_{35}=0$
SHX	$\dot{C}_{26}+\dot{C}_{28}+\dot{Z}_{\text{SHX}}=\dot{C}_{27}+\dot{C}_{29}$	$c_{28}=c_{29}$
Expansion valve 2	–	$c_{29}=c_{30}$
Pump 4	$\dot{C}_{26}=\dot{Z}_{\text{pump4}}+\dot{C}_{25}+\dot{C}_{w,\text{pump4}}$	$c_{w,\text{pump4}}=c_{w,\text{turb2}}$
Expansion valve 3	–	$c_{32}=c_{33}$
RO	$\dot{C}_{49}+\dot{Z}_{\text{RO}}+\dot{C}_{w,\text{RO}}=\dot{C}_{50}+\dot{C}_{51}$	$c_{w,\text{RO}}=c_{w,\text{turb1}},\ c_{49}=c_{51}=0$
PEM	$\dot{C}_{52}+\dot{C}_{w,\text{PEM}}+\dot{Z}_{\text{PEM}}=\dot{C}_{53}+\dot{C}_{54}$	$c_{w,\text{PEM}}=c_{w,\text{Exp}},\ c_{52}=0$

Table 3. Kalina cycle validation with the results of Ji-chao and Sobhani's work [17]

	T (K)		h (kJ/kg)	
Point	Ref. [17]	Present work	Ref. [17]	Present work
22	637.5	637.5	2480	2480
23	460.07	460.03	2126	2126
24	460.07	460.03	2279	2279
25	460.07	460.03	741.1	741.1
26	320.44	320.53	134.5	135.1
27	320.8	321.2	134.5	135.1
28	381.43	381.56	1986	1986
29	380.97	381.86	1801	1803
30	308.2	308.2	−72.66	−72.61
31	310.44	31.51	−45.63	−45.58
32	324.51	324.53	14.69	14.69

3.2 Transcritical CO_2 cycle validation

Simulation data for the transcritical CO_2 cycle were validated by comparing results reported by Wu et al. [18]. The simulation produced thermal efficiency and pressure-related performance results consistent with those observed in the Kalina cycle validation. Small differences, mainly at high temperature regions, arose due to differing heat exchanger designs and working fluid specifications used in each study's model. Overall, the results demonstrate strong agreement, confirming the suitability of our simulation code for modeling the transcritical CO_2 cycle. The comparison data are summarized in Table 4.

Table 4. Transcritical cycle validation with the results of Wu et al.'s work [18]

Parameter	Present work	Ref [18]
$\dot{Q}_{\text{LTR}}$ (kW)	453.83	436.36
$\dot{Q}_{\text{HTR}}$ (kW)	571.67	571.4
$\dot{W}_{\text{mc}}$ (kW)	76.13	76.09
$\dot{W}_{\text{RC}}$ (kW)	73.28	73.53
$\dot{W}_{\text{turb}}$ (kW)	393.18	393.24

The following conditions were established during combined cycle simulation:

- Exergy analysis is used to evaluate energy destruction under reference conditions defined by ambient temperature and pressure.
- The heat exchangers and their connected pipes experience no pressure reduction.
- Over time the system works at a steady state while keeping its continuous process equilibrium.
- System performance and efficiency depends on predetermined isentropic efficiency rates of pumps, turbines, and expanders.
- System behavior remains unaffected by the changes in energy between different cycle sections because these effects are considered negligible.

The data in Table 5 confirm that the system effectively generates electricity, hydrogen, and freshwater, as well as providing heating and cooling, while maintaining high overall energy efficiency and low emissions – supporting its integration into smart renewable energy networks.

Table 5. Overall energy, exergy and economic exergy results for the multigeneration system

The amount of power produced by the Kalina cycle (kW)	3289.6
The amount of power produced by the ORC cycle (kW)	2672.8
Total system produced work (kW)	5962.4
Overall exergy efficiency (%)	32.04
Electrical exergy efficiency (%)	11.65
Total exergy destruction of the system (kW)	24401.63
Production cooling rate (kW)	25549.12
Total cost rate of system exergy destruction ($/hr)	1781.52
Total cost rate of system equipment ($/hr)	1095.84
Overall economic exergy factor (%)	39.14
Total cost rate of the system($/hr)	2877.37
Cooling unit production cost ($/GJ)	25.8
Unit cost of electricity production ($/GJ)	90.6
Total system unit cost ($/GJ)	65.59
Hydrogen production rate (kg/s)	0.009
Freshwater production rate (kg/s)	7.998

Table 6. Energy, exergy and exergoeconomic results in different components of the proposed system

Component	$\dot{Q}$ or $\dot{W}$ (kW)	$\dot{E}x_D$ (kW)	η_{ex} (%)	$\dot{C}_D$ ($/hr)	$\dot{Z}_D$ ($/hr)
Turbine 1	3180.63	666.86	84.98	4.65	21.02
Turbine 2	8638.28	2545.33	79.4	148.96	57.61
Expander 1	257.72	69.54	80.96	0.48	1.59
Expander 2	2825.97	1178.09	72.56	261.42	946.99
Pump 1	144.54	25.96	84.35	0.39	1
Pump 2	52.53	13.09	77.18	8.5	0.99
Pump 3	315.49	166.95	48.39	13.76	3.55
Heat exchanger 1	25647.57	1076.32	87.36	5.03	1.84
Heat exchanger 2	5572.79	328.65	61.53	2.29	1.83
Heat exchanger 3	22353.86	674.57	73.71	9.19	1.57
Heat exchanger 4	19581.34	1201.73	29.78	81.52	2.24
Heat exchanger 5	19562.84	222.77	95.96	1.04	1.7
Heat exchanger 6	2584.39	150.4	50.76	0.7	1.61
Evaporator 1	6206.04	354.25	15.89	52.25	1.36
Evaporator 2	25549.91	737.18	70.4	93.92	28.71
Compressor	8638.28	2353.09	74.28	193.88	11.16
Gas cooler	19917.50	1220.24	12.9	152.56	9.16
Absorber	7702.8	353.43	16.53	44.34	0.47
Generator	8073.91	67.33	97.03	8.41	0.9
Condenser	6567.89	173.01	25.73	25.51	0.1
SHX	1517.33	45.23	72.78	5.97	0.2
Expansion valve 1	-	1286.03	-	163.86	-
PEM	-	36.046	29.93	14.59	44625
RO	-	73.54	36.45	100.9	10.5

A comprehensive breakdown of system component-level results includes energy, exergy, and exergoeconomic evaluations, is presented in Table 6.

The analysis highlights the locations of major system inefficiencies and associated financial costs. The highest exergy losses occur in Turbine 2, with 2,545.33 kW of exergy destruction, followed by the compressor at 2,353.09 kW, corresponding to costs of $148.96/hr and $193.88/hr, respectively. Turbine 1 demonstrates strong performance with an exergy efficiency of 84.98%. Heat Exchanger 4 and the Gas Cooler account for exergy losses of 1,201.73 kW and 1,220.24 kW, with exergy efficiencies of 29.78% and 12.9%, leading to economic costs of $81.52/hr and $152.56/hr, respectively. The Generator and Heat Exchanger 5 operate at a 97.03% efficiency rate with low related cost. Expansion Valve 1 exhibits an exergy destruction rate of 1,286.03 kW while producing no work, making it an optimal candidate for replacement with a more efficient expander system. The obtained results provide guidance for en-

gineers in optimizing system designs and developing retrofit plans to improve both efficiency and economic performance.

Figure 2 demonstrates the effects of cost rate and the variations in the economic exergy factor with increasing high pressure in the Kalina cycle. The system performance improves substantially when the high pressure rises from 4000 kPa to 4900 kPa because both exergy destruction cost rate (C_{des}) and total cost rate (C_{tot}) diminish. An increase in high pressure in the Kalina cycle reduces C_{des} from \$1912.08/h to \$1486.49/h while Ctot drops from \$3084.00/h to \$2464.12/h. An increase in high pressure leads the capital investment cost rate (Z_{tot}) to decrease from \$1171.92/h to \$922.12/h. The improved thermodynamic operation of Expander 3, along with Compressor functions and Heat Exchanger 4 performance, leads to reduced exergy destruction and related costs when operating at higher pressures. The system demonstrates improved economic efficiency at higher pressures when the economic exergy factor (ftot) registers a minor increase from 39.03% to 39.35%. An increase in system pressure enhances economic efficiency since the costs related to product creation take precedence over exergy destruction expenses.

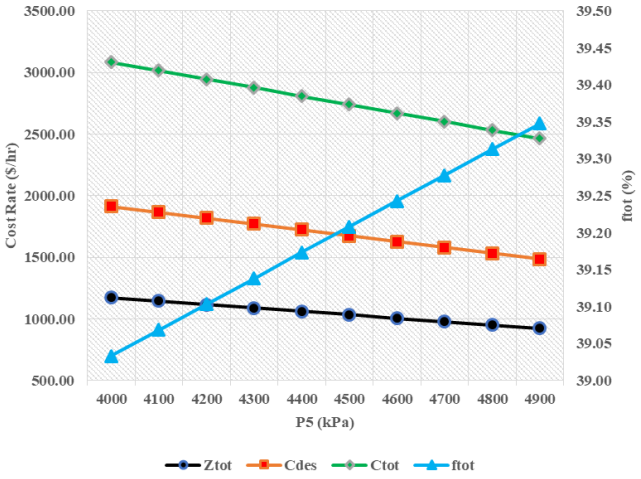

Fig. 2. The effect of Kalina cycle high pressure on the cost rates

According to Figure 3, the system costs decrease as the pinch temperature difference ($\Delta T_{\mathrm{pinchHX1}}$) in Heat Exchanger 1 becomes larger. Higher pinch temperature difference reduce exergy destruction across Heat Exchanger 4, Expander 3 and the Compressor which together decrease their financial costs. A substantial decrease in the exergy destruction cost rates occurs when operating the multi-generation system. The initial capital cost rate decreases primarily because Expander 3 requires less capacity when the pinch temperature difference is elevated. Further cost reductions and investment requirements lead to decreased exergy efficiency and reduced energy output as an important aspect for economic evaluation.

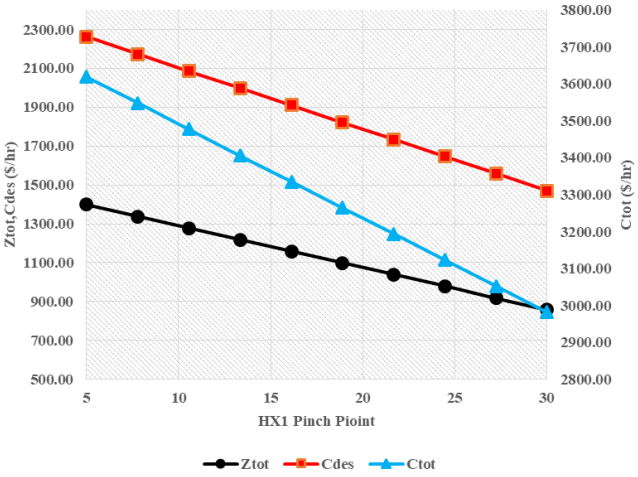

Fig. 3. The effect of heat exchanger 1 pinch point on the cost rates

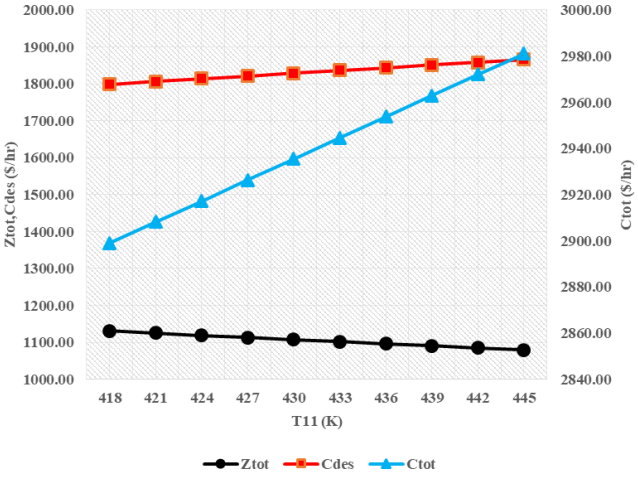

Fig. 4. The effect of separator temperature on the cost rates

Figure 4 illustrates how changes in the separator inlet temperature of the Kalina cycle affect system cost rates. As the inlet temperature increases, the initial cost rate decreases, mainly due to lower costs associated with Expander 3. However, the exergy destruction cost rate increases with higher temperatures, primarily due to greater inefficiencies in Heat Exchanger 2, which raises overall exergy destruction and associated costs. Consequently, the total cost rate rises as the separator temperature increases. For instance, the total cost rate increases from 2898.96 units at 418 °C to 2981.12 units at 445 °C. In summary, while the initial cost decreases with lower Expander 3 costs, the increased exergy destruction from Heat Exchanger 2 results in a higher overall cost, showing a dual effect of higher inlet

temperatures: reduced equipment costs but increased exergy destruction and system costs.

An increase in the ammonia mass fraction in the Kalina cycle improves both hydrogen and freshwater outputs (Figure 5). A rise in ammonia mass fraction enables the ORC to produce increased power which enhances improved PEM electrolyzer hydrogen production from 0.01167 kg/s to 0.01943 kg/s. Similarly, the RO desalination system produces more freshwater, increasing output from 6.861 kg/s to 8.414 kg/s. These gains enhance overall system performance but come at the expense of higher costs and increased design complexity.

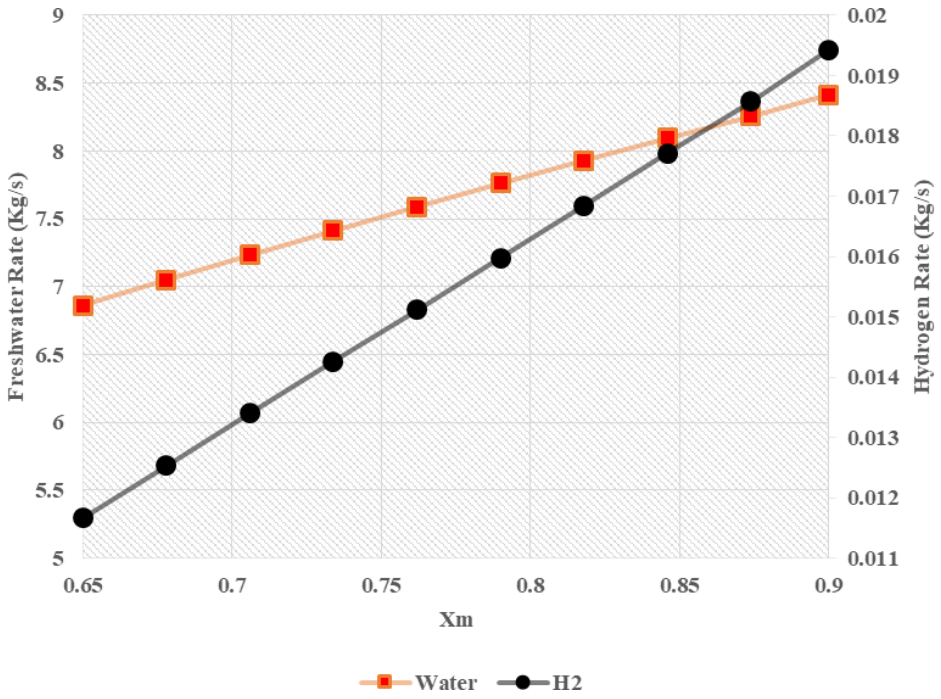

Fig. 5. The effect of mass fraction of ammonia on the amount of hydrogen and freshwater production rates

An increase in the absorber and condenser temperatures results in lower coefficient of performance (COP) in a single-effect absorption system according to Figure 6. When the absorber temperature is maintained at 303 K while the condenser temperature increases from 303 K to 313 K, the COP declines from 0.813 to 0.776. An increase in the temperature of either the absorber or the condenser results in corresponding COP reduction. The increase in the solution circulation ratio at elevated temperatures causes enhanced heat duty in the generator and greater pump work, resulting in a reduced COP.

System performance patterns are caused by the underlying principles of thermodynamics. When the high-pressure level in the Kalina cycle rises, the work output of the turbine and the overall efficiency both improve. This takes place because greater pressure enhances energy conversion efficiency in the cycle process. Variations in the ammonia mass fraction also significantly affect generating hydrogen and freshwater supply. Higher ammonia content enhances the performance of the Kalina and ORC systems, providing additional power to operate the PEM electrolyzer and RO desalination unit. These interactions between the subsystems in a multigeneration system maximize the use of available resources. Since Turbine 2 and Compressor handle most of the energy, the largest exergy destruction is expected to occur in these components. Examining these mechanisms helps researchers to identify improved strategies to optimize the system in the future.

4 Conclusion

A geothermal system using the Kalina cycle has been shown to provide heat, electricity, air conditioning, hydrogen, and freshwater with high productivity and low cost. Under optimal conditions, the system achieves a total efficiency of 47.6% and an exergy efficiency of 44.2%. Running the Kalina cycle at pressures between 4000 and 4900 kPa decreases exergy destruction cost to

$1486.49/h and brings down the overall system cost to $2464.12/h. A higher-pressure system results in lower investment costs per hour (from $1171.92 to $922.12), thereby improving the project's economic efficiency. Among all the equipment, the greatest exergy destruction resulted from the Compressor and Turbine 2, with the values of 2545.33 kW and 2353.09 kW, respectively. Alternatively, the Generator and Heat Exchanger 5 maintain exergy efficiency of 97.03%, contributing to energy savings within the system. The sequences can also supply 30,178 kW of electricity and 3498 kW of cooling. Production of hydrogen at the plant is 0.1524 kg/h, comparable to that of other geothermal multi-generation facilities. Although clean hydrogen output may be lower compared to other fuels, utilizing larger or higher-temperature sources can enhance its contribution to sustainability and increase its practical utility. It can be used to power vehicles or help balance the electricity grid. Overall, integrating the Kalina cycle with geothermal energy and well-designed components enables efficient energy recovery at a reasonable cost. In the next phase, pilot-scale experiments will be conducted to verify performance and fine-tune the model, improving confidence in the system's design.

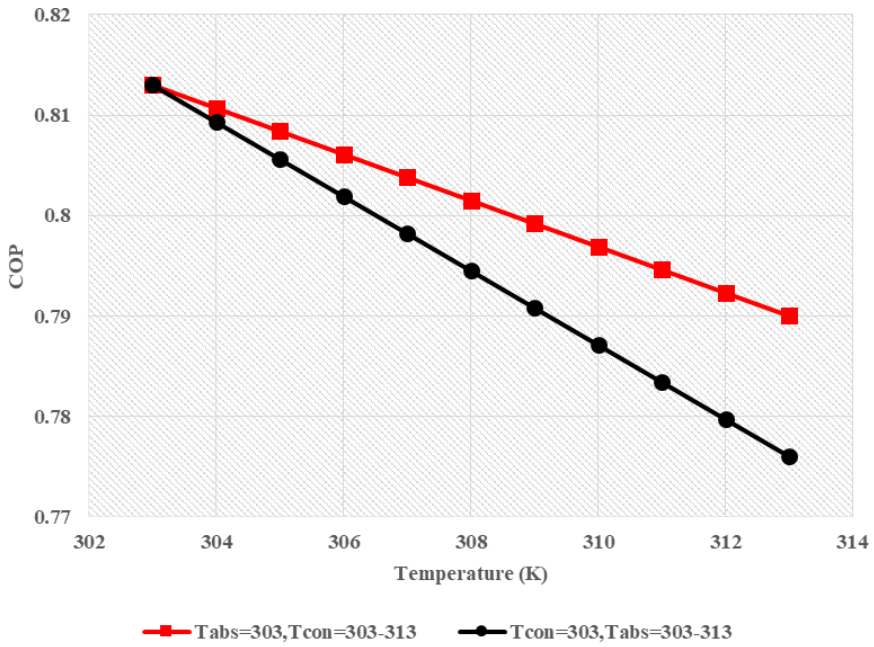

Fig. 6. Effect of Absorber and Condenser Temperature Difference on COP

Nomenclature

C_{des}	Exergy destruction cost rate	$/h
C_{tot}	Total cost rate of the system	$/h
Z_{tot}	Capital investment cost rate	$/h
f_{tot}	Economic exergy efficiency factor	-
P	Pressure	kPa
T	Temperature	K
$\dot{m}_{\text{H}_2}$	Hydrogen production rate	kg/s
$\dot{Q}$	Heat transfer rate	kW
η_{energy}	Energy efficiency	%
η_{exergy}	Exergy efficiency	%
h	Enthalpy	kJ/kg
s	Entropy	kJ/kgK
$\dot{W}$	Power output	kW
COP	Coefficient of performance (for refrigeration)	-
$\dot{V}$	Volumetric flow rate	m^3/h or Nm^3/h
$\dot{m}$	Mass flow rate	kg/s

References

[1] Lund JW, Boyd TL. Direct utilization of geothermal energy 2015 worldwide review. Geothermics. 2016;60:66-93.

[2] Nassir AK, Shahad HA. Retraction: Kalina cycle system (a state of the art). In: AIP Conference Proceedings. vol. 2977. AIP Publishing LLC; 2023. p. 030018.

[3] Azariyan H, Vajdi M, Takleh HR. Assessment of a high-performance geothermal-based multigeneration system for production of power, cooling, and hydrogen: Thermodynamic and exergoeconomic evaluation. Energy Conversion and Management. 2021;236:113970.

[4] Bejan A, Tsatsaronis G, Moran MJ. Thermal design and optimization. John Wiley & Sons; 1995.

[5] Kaczmarczyk M, Tomaszewska B, Pająk L. Geological and thermodynamic analysis of low enthalpy geothermal resources to electricity generation using ORC and Kalina cycle technology. Energies. 2020;13(6):1335.

[6] Hai T, Lin H, Chauhan BS, Ayed H, Loukil H, Galal AM, et al. Performance analysis and optimization of a novel geothermal trigeneration system with enhanced Organic Rankine cycle, Kalina cycle, reverse osmosis, and supercritical CO_2 cycle. Renewable Energy. 2023;211:539-62.

[7] Bahrami HR, Rosen MA. Exergoeconomic evaluation and multi-objective optimization of a novel geothermal-driven zero-emission system for cooling, electricity, and hydrogen production: capable of working with low-temperature resources. Geothermal Energy. 2024;12(1):12.

[8] Bahrami HR, Rosen MA. Exergoeconomic evaluation and multi-objective optimization of a novel geothermal-driven zero-emission system for cooling, electricity, and hydrogen production: capable of working with low-temperature resources. Geothermal Energy. 2024;12(1):12.

[9] Musharavati F, Ahmadi P, Khanmohammadi S. Exergoeconomic assessment and multiobjective optimization of a geothermal-based trigeneration system for electricity, cooling, and clean hydrogen production. Journal of Thermal Analysis and Calorimetry. 2021;145(3):1673-89.

[10] Ambriz-Diaz VM, Chavez O, Rosas IY, Godinez F. 4E feasibility analysis of a low-emissions multigeneration system operating at different hierarchical levels in geothermal cascade. Journal of the Brazilian Society of Mechanical Sciences and Engineering. 2024;46(6):351.

[11] Xu J, Su Z, Meng J, Yao Y, Vafadaran MS, Salavat AK. A thermodynamic, exergoeconomic, and exergoenvironmental investigation and optimization on a novel geothermal trigeneration system to sustain a sport arena. Process Safety and Environmental Protection. 2023;177:278-98.

[12] Kelem UR, Yilmaz F. An innovative geothermal based multigeneration plant: thermodynamic and economic assessment for sustainable outputs with compressed hydrogen. Energy. 2024;295:131084.

[13] Singh KK, Kumar R, Gupta A. Comparative exergetic, economic and exergoeconomic analyses of a hybrid cascade refrigeration system using ammonia-propane, propane-propylene and isobutane-propane refrigerant pairs. International Journal of Exergy. 2021;36(2-4):315-29.

[14] Abdolalipouradl M, Khalilarya S, Jafarmadar S. Exergoeconomic analysis of a novel integrated transcritical CO_2 and Kalina 11 cycles from Sabalan geothermal power plant. Energy Conversion and Management. 2019;195:420-35.

[15] Dong RE, Zhanguo S, Mansir IB, Abed AM, Niu X. Energy and exergoeconomic assessments of a renewable hybrid ERC/ORC integrated with solar dryer unit, PEM electrolyzer, and RO desalination subsystem. Process Safety and Environmental Protection. 2023;171:812-33.

[16] Kianfard H, Khalilarya S, Jafarmadar S. Exergy and exergoeconomic evaluation of hydrogen and distilled water production via combination of PEM electrolyzer, RO desalination unit and geothermal driven dual fluid ORC. Energy conversion and management. 2018;177:339-49.

[17] Ji-chao Y, Sobhani B. Integration of biomass gasification with a supercritical CO_2 and Kalina cycles in a combined heating and power system: a thermodynamic and exergoeconomic analysis. Energy. 2021;222:119980.

[18] Hai T, Aziz KHH, Zhou J, Dhahad HA, Sharma K, Almojil SF, et al.. RETRACTED: Neural network-based optimization of hydrogen fuel production energy system with proton exchange electrolyzer supported nanomaterial. Elsevier; 2023.